Theor Chem Acc (2011) 128:165–174
DOI 10.1007/s00214-010-0808-5

REGULAR ARTICLE

Theoretical investigation into optical and electronic properties of oligothiophene derivatives with phenyl ring as core or end-capped group in linear and V-shape

Shanshan Tang · Jingping Zhang

Received: 16 April 2010 / Accepted: 27 August 2010 / Published online: 11 September 2010

Abstract A series of thiophene-based oligomers has been designed to explore their optical, electronic, and charge transport properties for charge transport materials. These oligomers consist of oligothiophene, oligo(thienylenevinylene), and *m*- or *p*-phenyl as the core in two shapes (linear shape and V-shape). Phenyl ring as the end-capped group is also investigated in the linear shape. The DFT-PBE0/6-31G(d,p) and the TD-PBE0/6-31+G(d,p) calculated results reported herein show that the V-shape oligomers have larger HOMO-LUMO gaps because of meta-substitutions on phenyl cores, corresponding to blue shifts of absorption spectra. The linear oligomers with phenyl ring as end-capped group display red shifts of absorption spectra. The V-shape oligomers provide small reorganization energies. Our recommended polymer possessing 1,2,4-phenyl core and longer OTV side fragments is a good candidate for the design of charge transport and/or solar cell materials.

Keywords Oligothiophene derivatives · Optical and electronic properties · Charge transport property

Electronic supplementary material The online version of this article (doi:10.1007/s00214-010-0808-5) contains supplementary material, which is available to authorized users.

S. Tang · J. Zhang (✉)
Faculty of Chemistry, Northeast Normal University, 130024 Changchun, China
e-mail: zhangjingping66@yahoo.com.cn

S. Tang
College of Resource and Environmental Science, Jilin Agricultural University, 130118 Changchun, China

1 Introduction

Organic materials used as optical and electronic devices, such as organic light-emitting diodes (OLEDs), organic field-effect transistors (OFETs), and organic solar cells (OSCs), have recently received a great deal of attention from the standpoint of potential technological applications as well as fundamental science [1–24]. The devices using organic materials are attractive because of their excellent properties, for example, light weight, potentially low cost, capability of thin-film, large-area, and flexible device fabrication.

Functional thiophene-related oligomers and polymers have drawn much attention because they are the most frequently used π-conjugated systems among organic materials, particularly as active components in organic electronic devices and molecular electronics [25–28]. Many substituted derivatives have been designed and synthesized, and their optical and electronic properties have also been investigated [29–42]. Recently, the traditional linear systems have been vastly extended to higher dimensionalities and novel topologies [43]. It is well known that charge transport property in organic materials is one of the most important properties in the performance of OLEDs [44, 45], OFETs [46, 47], and OSCs [48–50]. Understanding the relationship between the two different molecular shapes and charge transport property of a material is a key factor for providing the guideline for device design, and great theoretical research efforts are currently being made in this regard [51–53].

With the aim to explore the detail of the two different molecular shapes for charge transport and/or solar cell applications of well-investigated oligothiophene (OT) and oligo(thienylenevinylene) (OTV), we designed three series

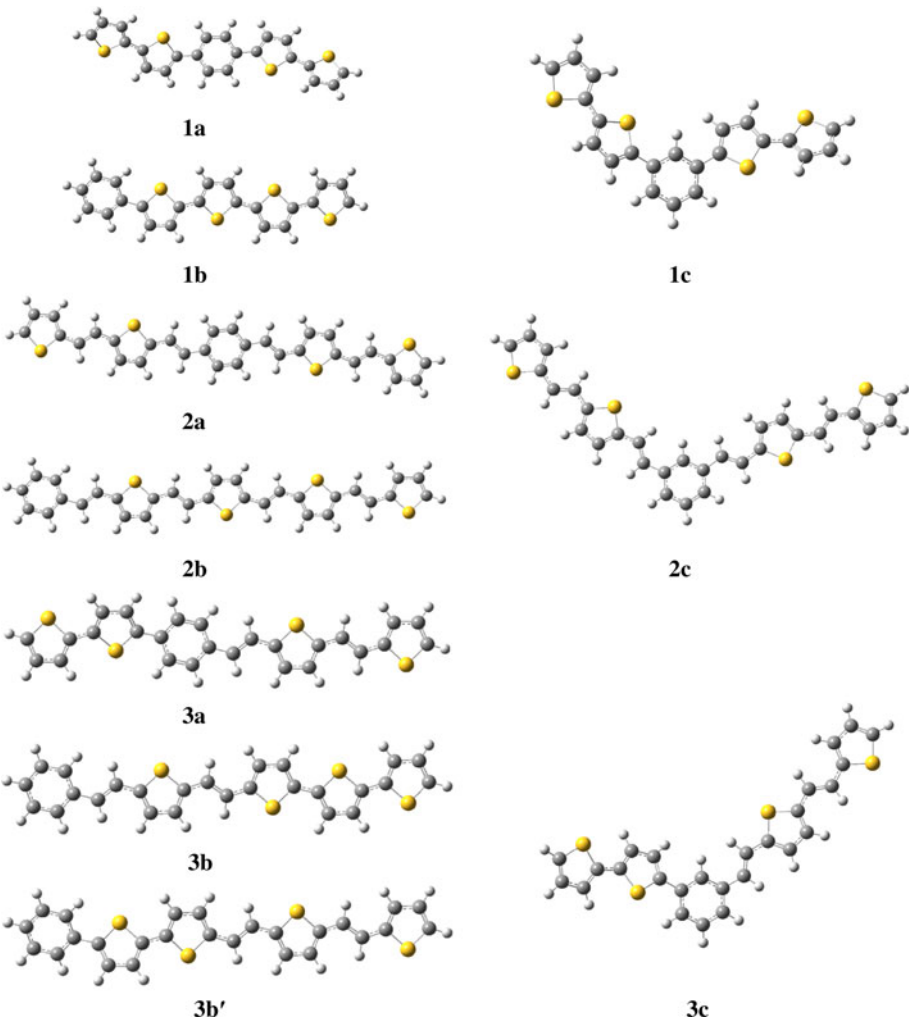

Fig. 1 Molecular structures of the investigated molecules

of OT and OTV derivatives by introducing phenyl ring as core or end-capped group forming two topologies, i.e., linear or V-shape (see Fig. 1). For understanding the effects of the position of phenyl ring and the two different molecular shapes for OT derivatives on their optical and electronic properties, the first series is obtained as follows: (1) **1a** corresponds to the linear OT with *p*-phenyl as core; (2) **1b** refers to the linear OT with phenyl ring as end-capped group; (3) **1c** is the V-shape OT with *m*-phenyl as core. The second series (**2a–c**) is considered for investigating the influence of the position of phenyl ring and the two different molecular shapes of OTV derivatives on their optical and electronic properties. To study the properties for co-oligomers of oligothiophene-phenyl-oligo(thienylenevinylene), **3a–c** were designed. The frontier molecular orbitals (FMOs) including the highest occupied molecular orbital (HOMO) and the lowest unoccupied molecular orbital (LUMO) energies, the HOMO–LUMO gaps (E_g) as well as the absorption spectra were predicted. According to the Marcus model [54–56], there are two key parameters for charge transfer rate which are electronic coupling matrix element and reorganization energy, and the latter is more important [57]. Hence, we mainly study the reorganization energy for electron (λ_e) and hole (λ_h) of the designed molecules to investigate their charge transport properties. In addition, the correlations between these properties and their molecular topologies were also discussed. On the basis of detailed investigation of designed oligomers, the most promising candidates were designed as **4a–f** (Scheme 1); the various properties of corresponding polymer were predicted by extrapolation technique.

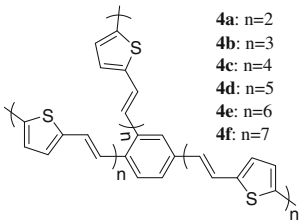

Scheme 1 Chemical structures of **4a–f** as the most promising candidates

2 Computational details

All the calculations were carried out with the aid of Gaussian 03 package [58]. The density function theory (DFT) [59] with the PBE0 [60, 61] method using the 6-31G(d,p) [62–64] basis set was selected in all the geometry optimization including neutral, cation, and anion molecules. Our previous work [65] and the reports by Jacquemin [66–69] suggested that the PBE0 appeared notably adapted to sulfur-bearing molecules. Molecules **1a** and **2a** possess C_2 symmetries. Considering the fact that oligothiophene is flat in crystal [70], **1a′**–**c′** are restricted in planar conformation in comparison with **1a**–**c**, respectively (see Fig. S1, Supporting Information). **1c** and **2c** are more stable ones in their possible conformations, respectively, (see Fig. S1 and Table S1, Supporting Information). The absorption spectra of all the compounds were investigated by the TD-PBE0/6-31+G(d,p) [64, 71–75] method based on the optimized geometries at the PBE0/6-31G(d,p) level. To investigate the solvent effects on the optical and electronic properties of the derivatives, we adopted the self-consistent reaction field (SCRF) approach with the polarizable continuum model (PCM) [62, 76–81] using benzene, acetonitrile, and chloroform solvents to calculate the absorption spectra of **1a** as representation. Recently, the B3LYP/6-31G(d,p) [82] functional was successfully used to calculate charge transport parameters for OT [83]. Moreover, in order to compare with the interested results reported previously [84, 85], the reorganization energies for electron (λ_e) and hole (λ_h) of the molecules were predicted from the single point energy at the B3LYP/6-31G(d,p) level on the basis of the PBE0/6-31G(d,p) optimized neutral, cationic, and anionic geometries. The reorganization energy can be divided into two parts, external reorganization energy (λ_{ext}) and internal reorganization energy (λ_{int}). λ_{ext} represents the effect of polarized medium on charge transfer; on the other hand, λ_{int} is a measure of structural change between ionic and neutral states [86]. In the solid-state film of charge transport and/or solar cell materials, λ_{ext} is not expectable to be the main factor of reorganization energy, because of the low dielectric constant of medium [87]. Therefore, we focus the discussion on the internal reorganization energy of the isolated active organic π-conjugated systems due to ignoring any environmental relaxation and changes in this paper. Hence, the λ_e and λ_h values can be calculated by Eqs. 1 and 2 [88]:

$$\lambda_e = \left[E_0^- - E_-\right] + \left[E_-^0 - E_0\right] \quad (1)$$

$$\lambda_h = \left[E_0^+ - E_+\right] + \left[E_+^0 - E_0\right] \quad (2)$$

Where $E_0{}^+$ ($E_0{}^-$) is the energy of the cation (anion) calculated with the optimized structure of the neutral molecule. Similarly, E_+ (E_-) is the energy of the cation (anion) calculated with the optimized cation (anion) structure, E_+^0 (E_-^0) is the energy of the neutral molecule calculated at the cationic (anionic) state. Finally, E_0 is the energy of the neutral molecule at the ground state. The B3LYP/6-31G(d,p) level was also used for the solvent reorganization energies of electron and hole for **1a** in benzene, chloroform, and acetonitrile solvents, respectively, using PCM models as representation. The density of states (DOS) was calculated and convoluted using the Gausssum 1.0 [89].

3 Results and discussion

3.1 Molecular structures

In general, the comparison of the optimization results for three fragments (thiophene, phenyl ring, and thienylene-vinylene) of investigated molecules does not reveal any significant change in the geometry of the skeleton. The main structural changes occurred between the adjacent units, especially the geometrical parameters between phenyl ring and thiophene fragments. The molecular structures are presented in Scheme S1 (see the Supporting Information), and the calculated results have been listed in Table 1. For OT

Table 1 Optimized geometrical parameters for the structures of molecules

Species	Geometrical parameters			
1a	m_{2-7} (Å) 1.46	m_{5-9} (Å) 1.46	$\alpha_{3-2-7-8}$ (°) 22	$\alpha_{6-5-9-10}$ (°) 22
1b	m_{2-7} (Å) 1.46		$\alpha_{3-2-7-8}$ (°) 27	
1c	m_{2-7} (Å) 1.46	m_{6-9} (Å) 1.46	$\alpha_{3-2-7-8}$ (°) 28	$\alpha_{1-6-9-10}$ (°) 27
2a	m_{2-7} (Å) 1.45	m_{5-9} (Å) 1.45	$\alpha_{1-2-7-8}$ (°) 2	$\alpha_{4-5-9-10}$ (°) 2
2b	m_{2-7} (Å) 1.46		$\alpha_{1-2-7-8}$ (°) 0	
2c	m_{2-7} (Å) 1.46	m_{6-9} (Å) 1.46	$\alpha_{1-2-7-8}$ (°) 2	$\alpha_{5-6-9-10}$ (°) 0
3a	m_{2-7} (Å) 1.46	m_{5-9} (Å) 1.45	$\alpha_{1-2-7-8}$ (°) 13	$\alpha_{6-5-9-10}$ (°) 0
3b	m_{2-7} (Å) 1.46		$\alpha_{1-2-7-8}$ (°) 0	
3b′	m_{2-7} (Å) 1.46		$\alpha_{3-2-7-8}$ (°) 27	
3c	m_{2-7} (Å) 1.46	m_{6-9} (Å) 1.46	$\alpha_{1-2-7-8}$ (°) 30	$\alpha_{1-6-9-10}$ (°) 12

Bond lengths (m) and bond angles (α) are listed

derivatives, both the two inter-ring distances between phenyl ring and thiophene fragments of **1a** are 1.46 Å. Its inter-ring dihedral angles are 22°, which is due to the steric hindrances. For **1b**, the inter-ring distances between phenyl ring and thiophene fragments are similar to those of **1a**, and its inter-ring dihedral angles are larger than those of **1a**. This indicates that different positions of phenyl ring have effects on the geometry parameters of OT derivatives. However, the inter-ring dihedral angles between phenyl ring and thiophene fragments of **1c** are increased to 28° and 27°, respectively, while the inter-ring instances have no obvious changes. It is because of larger steric hindrance in meta-substitution than that in para-substitution. The inter-ring distances of **1a′**–**c′** are similar (with the deviations less than 0.02 Å) to those of **1a**–**c**, respectively. For OTV derivatives, the inter-ring distances and dihedral angles between phenyl ring and thienylenevinylene fragments of **2a**–**c** are similar, which are about 1.45 Å and 2°, respectively. Therefore, the geometry parameters of OTV derivatives are only slightly influenced by the position of phenyl ring and the two different molecular shapes. For co-oligomers (**3a**–**c**), the inter-ring distances and dihedral angles between phenyl and thiophene fragments are similar to those of **1a**, and the inter-ring distances and dihedral angles between phenyl and thienylenevinylene fragments are slightly larger than those of **2a**. Hence, the positions of phenyl ring and the two different molecular shapes have slight effects on the inter-ring distances for OT, OTV derivatives, and co-oligomers. While the inter-ring dihedral angles of OT and co-oligomer derivatives depend on their molecular shapes, V-shape molecules have larger inter-ring dihedral angles than linear ones (see Table 1) because of meta-substitution possessing larger steric hindrance than that of para-substitution.

3.2 Frontier molecular orbitals

To characterize the optical transitions and the abilities of electron and hole transport, we calculated the distribution patterns of FMOs for all the investigated molecules (see Figs. 2 and S2). For a more detailed comparative study of the electronic structures, the total density of states (TDOS) and projected partial density of states (PDOS) on each fragment of the investigated molecules were calculated based on the current level of theory, as shown in Figs. 3 and S3.

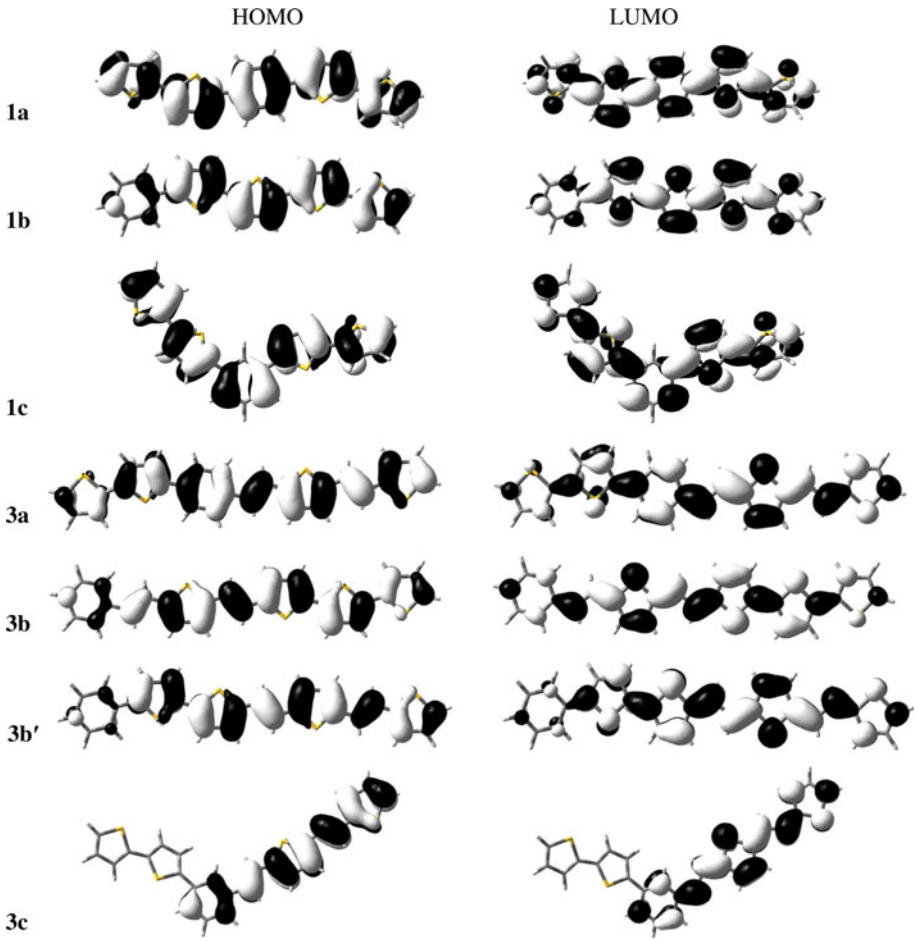

Fig. 2 The FMOs of the investigated molecules at the PBE0/6-31G(d,p) level

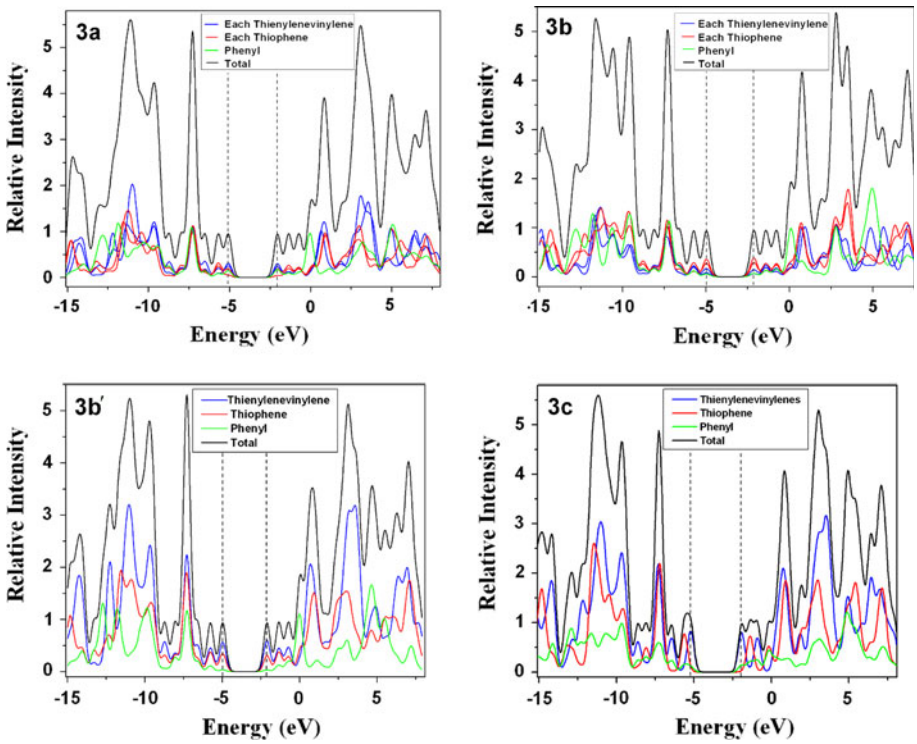

Fig. 3 Total and partial density of states (TDOS and PDOS) around the HOMO–LUMO gap for investigated molecules (the value of full width at half maxima (FWHM) is 0.3 eV, *dashed vertical lines* indicate the HOMO and LUMO energies, respectively)

The origin of the geometric difference introduced by excitation can be explained, at least in qualitative terms, by analyzing the change in the bonding character of the orbitals involved in the electronic transition for each pair of bonded atoms [90]. As shown in Figs. 2 and S2, the ground state (S_0) → first singlet excited state (S_1) excitation process can be mainly assigned to the HOMO → LUMO transition, which corresponds to a π–π^* excited singlet state. From Figs. 2 and S3, one can find that the FMOs of **1a** and **1c** are composed of contributions of the phenyl rings and thiophene fragments. For **1b**, the FMOs are highly delocalized throughout the thiophene fragments, with minor contributions from phenyl ring. The results of **1a′**–**c′** are similar to those of **1a**–**c** (see Figs. S2 and S3, Supporting Information). The FMOs of **2a** and **2c** are fairly distributed on the phenyl ring and thienylenevinylene fragments. For **2b**, the contributions from phenyl ring are smaller than those of thienylenevinylene fragments. These results reveal that the distribution patterns of FMOs for OT and OTV derivatives are influenced slightly by the position of phenyl ring and the two different molecular shapes. The contributions of HOMO and LUMO are only minor from one thiophene fragment (5% for HOMO and 4% for LUMO) for **3a**. Its phenyl ring (15% for HOMO and 19% for LUMO) and the other thiophene fragment (20% for HOMO and 20% for LUMO) offer small contributions, and two thienylenevinylene fragments have large contributions (60% for HOMO and 57% for LUMO). For **3b**, the contributions of phenyl ring and thienylenevinylene fragments in FMOs are smaller than those of **3a**, and the contributions from thiophene fragments are larger than those of **3a**, respectively. For **3b′**, the contributions of phenyl ring in FMOs are smaller than those for **3a**, whereas the contributions coming from thienylenevinylene fragments are similar to those of **3a**, and the contributions by thiophene fragments are larger than those of **3a** in FMOs, respectively. These results show that the distribution patterns of FMOs are influenced slightly by the position of phenyl ring for linear co-oligomers. It is worth noting that the FMOs of **3c** have nearly no contributions from the thiophene fragments. The contributions from the phenyl ring are small in FMOs of **3c** (11% for HOMO and 15% for LUMO), and the contributions from thienylenevinylene fragments are dominant (88% for HOMO and 85% for LUMO). Therefore, various molecular topologies should influence significantly the distribution patterns of FMOs for co-oligomers.

For a better understanding of the effects of the position of phenyl ring and the two different molecular shapes on the energies of FMOs, we calculated HOMO and LUMO energies (E_{HOMO} and E_{LUMO}), and the evaluations are schematically shown in Fig. S4 (see the Supporting Information). The calculated results reveal that for OT derivatives, the V-shape OT derivative (**1c**) has lower E_{HOMO} and higher E_{LUMO} and E_g values than those of linear ones (**1a** and **1b**). The similar tendency can be also found for **1a′**–**c′** (see Table S2, Supporting Information). As shown in Fig. S4, OTV derivatives with phenyl ring as core (**2a** and **2c**)

have larger E_g values than that of the one with phenyl ring as end-capped group (**2b**). For co-oligomers, the molecules with phenyl ring as end-capped group (**3b** and **3b′**) have higher E_{HOMO} and lower E_{LUMO} and E_g values than those with phenyl ring as core (**3a** and **3c**). As a result, the stabilization of the HOMO or LUMO depends on the position of phenyl ring and the two different molecular shapes, and the linear OTV with phenyl ring as end-capped group results in the smallest E_g value. The V-shape molecules have higher ionization potential (IP) and lower electron affinity (EA) values than those corresponding linear ones (see Table S3, Supporting Information), which are in line with the corresponding orders of absolute values for FMOs, respectively, as shown in Fig. S4 (see the Supporting Information).

3.3 Absorption spectra

The longest wavelength of maximal absorption (λ_{max}) and corresponding oscillator strength (f) of the investigated molecules at the TD-PBE0/6-31+G(d,p) level are listed in Table 2. For OT derivatives, the calculated λ_{max} values show the increasing order of **1c** < **1a** < **1b**, which is in good accordance with the corresponding reverse order of E_g values as shown in Sect. 3.2. A good agreement can be observed between our calculated λ_{max} value (414.81 nm) of **1a** and experimental observation (401.00 nm) [91]. This reveals that the level of theory we selected is reasonable for this kind of system. The predicted λ_{max} values of **1a** in different solvents are shown in Table S4 (see the Supporting Information). One can find that the deviations between different solvents are less than 16 nm. Therefore, different solvents (polar and non-polar) at PCM level have only slight effects on λ_{max} values. The order of corresponding f values is **1c** < **1b** < **1a**. The λ_{max} values of **1a′**–**c′** are predicted in the increasing order of **1c′** < **1a′** < **1b′**, and their corresponding f values are in sequence of **1c′** < **1b′** < **1a′** (see Table S2, Supporting Information). The λ_{max} value of **1a′**/**1b′**/**1c′** is larger than that of **1a**/**1b**/**1c**, respectively, due to its corresponding smaller E_g value. This indicates that OT derivatives will have large λ_{max} values in solid states due to their flat structures. For OTV derivatives, the λ_{max} values of **2a**–**c** are in the increasing order of **2c** < **2a** < **2b**, and their corresponding f values are in the sequence of **2c** < **2b** < **2a**. It suggests that OTV derivatives with phenyl ring as core (**2a** and **2c**) have smaller λ_{max} values than the one with phenyl ring as end-capped group (**2b**). The λ_{max} value of **2a**/**2b**/**2c** is larger than that of **1a**/**1b**/**1c** due to the smaller E_g value for **2a**/**2b**/**2c** in comparison with **1a**/**1b**/**1c**, respectively. For co-oligomers, the λ_{max} values are in the sequence of **3c** < **3a** < **3b′** < **3b**, their predicted f values in absorption spectra are found in increasing order of **3c** < **3b** < **3b′** < **3a**. These results show that the co-oligomers with phenyl ring as end-capped group (**3b** and **3b′**) have larger λ_{max} values than those possessing phenyl ring as core (**3a** and **3c**). The λ_{max} value of **3b** is close to that of **3b′** because of their similar distribution patterns of FMOs (Fig. 2). Furthermore, the V-shape co-oligomer (**3c**) has smaller λ_{max} value than those of linear ones. The λ_{max} and corresponding f values of co-oligomers are in between of those for corresponding OT and OTV derivatives, respectively. The calculated results reveal that V-shape molecules have smaller λ_{max} and corresponding f values than those linear shape molecules. This is ascribed to the meta-substitution inducing poor conjugation in comparison with para-substitution, which leads to V-shape molecules having larger E_g, smaller λ_{max}, and corresponding f values than linear ones. This result is in good agreement with earlier experimental observations [92, 93] and theoretical investigation (at the B3LYP/6-31G(d) level) [87] for similar systems. Moreover, the linear OTV derivative with phenyl ring as end-capped group (**2b**) has the largest λ_{max} value possessing more intensive spectrum.

Table 2 A comparative study of the predicted λ_{max} (nm) and corresponding f values for investigated molecules obtained at the TD-PBE0/6-31+G(d,p)//PBE0/6-31G(d,p) level and available experimental datum

Species	Main assignment	λ_{max}	f	Exp[a]
1a	H → L (0.65)	414.81	1.59	401.00
1b	H → L (0.65)	442.46	1.52	
1c	H − 1 → L (0.50)	358.01	1.29	
	H → L (0.15)			
	H → L + 1 (0.40)			
2a	H → L (0.64)	531.18	3.27	
2b	H → L (0.63)	557.51	3.24	
2c	H − 1 → L (0.49)	453.07	2.78	
	H → L + 1 (0.41)			
3a	H → L (0.64)	477.93	2.52	
3b	H → L (0.63)	512.99	2.42	
3b′	H → L (0.63)	505.94	2.45	
3c	H → L (0.62)	432.92	1.96	
	H − 1 → L + 1 (0.12)			

[a] Experimental datum of **1a** from Ref. [91]

3.4 Charge transport properties

Understanding the relationship between the two different molecular shapes and charge transport property of materials is a key point in providing good candidates for the design of charge transport and/or solar cell materials. The lower the reorganization energy value is, the higher the charge transfer rate is [94]. The calculated results for hole and electron according to Eqs. 1 and 2 are summarized in Table 3.

Table 3 Calculated molecular λ_e and λ_h (eV) values

Species	λ_e	λ_h
1a	0.328	0.340
1b	0.344	0.332
1c	0.268	0.239
2a	0.228	0.234
2b	0.261	0.271
2c	0.152	0.161
3a	0.276	0.288
3b	0.259	0.272
3b′	0.299	0.293
3c	0.276	0.261

The calculated internal reorganization energies of **1a** for electron (λ_e) and hole (λ_h) are 0.328 and 0.340 eV in gas, respectively (see Table 3). The corresponding λ_e and λ_h values of **1a** in various solvents are shown in Table S5 (see the Supporting Information). It shows that the deviations of λ_e and λ_h values for **1a** in different solvents are in the range of 0.013–0.048 eV and 0.007–0.037 eV, respectively. Therefore, different solvents (both polar and non-polar) at PCM level used in this study only slightly affect the reorganization energies, i.e., the reorganization energies are solvent independent. Similar performance has been reported previously [95]. Thus, in this work, the solvent effect for reorganization energy has been neglected. For OT derivatives, the calculated λ_e and λ_h values of **1a** are close to those of **1b**, respectively. Thus, different positions of phenyl rings should have slight effects on the charge transfer rates for linear OT derivatives in the same environment. However, the λ_e and λ_h values of **1c** are much lower than those of **1a** and **1b**, respectively. We explain this result by following the two facts: the effective overall overlap of HOMO and LUMO for **1a** and **1b** are smaller than that of **1c** (see Fig. 2) resulting in smaller λ_e and λ_h values of **1c** than those of **1a** and **1b** [96]; the smaller geometry relaxation between ions and neutral geometrical structures occurs in the phenyl core for **1c** than that for **1a** and **1b** [97] (see Scheme S1 and Table S6, Supporting Information), respectively. For example, for **1c**, the geometrical structure differences between the cation and neutral one in the bond lengths of the phenyl groups are in the range of 0–0.01 Å. In the case of **1a** and **1b**, a range of 0.01–0.03 Å is observed. Therefore, the intrinsic charge transport properties for investigated OT derivatives should be molecular shape dependent, namely the V-shape OT derivative with *m*-phenyl core (**1c**) should have higher charge transfer rate than that of linear ones (**1a** and **1b**) in the same environment. The λ_e values are 0.224, 0.243, and 0.159 eV for **1a′**–**c′**, and their λ_h values are 0.250, 0.263, and 0.174 eV, respectively. The λ_e and λ_h values of **1a′**–**c′** are smaller than those of **1a**–**c**, respectively. Thus, OT derivatives should have higher charge transfer rates in solid states because of their flat structures (considering the same environment). For OTV derivatives, the λ_e and λ_h values of **2a**–**c** are in the increasing sequence of **2c** < **2a** < **2b**. Moreover, the difference of λ_e values between **2a** and **2b** is 0.033 eV, and the difference of their λ_h values is 0.037 eV. The λ_e and λ_h values of **2c** are much lower than those of **2a** and **2b**, respectively, due to the same reasons as in **1a**–**c**. These results indicate that the charge transfer rates of OTV derivatives in linear shape are influenced slightly by the position of phenyl ring ignoring any environmental relaxation and changes. However, the different molecular topologies have significant effects on the charge transfer rates of OTV derivatives, that is, the V-shape OTV derivative (**2c**) should provide higher charge transfer rate than those of linear ones (**2a** and **2b**) in the same environment. The λ_e and λ_h values of **2a/2b/2c** are smaller than those of **1a/1b/1c**, respectively, implying OTV derivatives possessing higher charge transfer rates than those of OT derivatives considering the same environment. For co-oligomers, the calculated λ_e and λ_h values of **3a**–**c** are similar, indicating the position of phenyl ring and the two different molecular shapes having only a slight influence on λ_e and λ_h values. The calculated values of λ_e for **1c**, **2a**–**c**, and **3b** are lower than that of tris(8-hydroxyquinolinato) aluminum (III) (Alq3) ($\lambda_e = 0.276$ eV) [84] which is a typical electron transport material. This implies that their electron transfer rates might be higher than that of Alq3. Meanwhile, the values of λ_h for **1c**, **2a**–**c**, **3a**, **3b**, and **3c** are lower than that of *N*,*N*′-diphenyl-*N*,*N*′- bis(3-methlphenyl)-(1,1′-biphenyl)-4,4′-diamine (TPD) ($\lambda_h = 0.290$ eV) [85], which is a typical hole transport material. This indicates that their hole transfer rates might be higher than that of TPD. In addition, the differences between λ_e and λ_h for the investigated molecules do not exceed 0.029 eV, implying better equilibrium properties for hole- and electron-transport. Therefore, these molecules can be used as good candidates for ambipolar charge transport materials under the proper operating conditions. It is worth mentioning that the V-shape OTV derivative with *m*-phenyl core (**2c**) shows the lowest λ_e and λ_h values among the investigated molecules. Hence, it is the best candidate for charge transport materials among the investigated molecules.

3.5 The properties of corresponding polymer based on appreciated oligomers by extrapolation

Considering the optical and electric properties for designed molecules above, the rational way to designing molecules toward charge transport materials should possess 1,2,4-phenyl core and OTV side fragments (**4a**–**f**, as shown in Scheme 1). The *m*-phenyl contributes to higher charge

transfer rate considering the same environment; meanwhile, *p*-phenyl as well as OTV fragments contribute to the better optical property. To predict the optical and electronic properties of corresponding polymer, we studied oligomers **4a–f** (Scheme 1). The HOMO, LUMO, E_g, λ_{max}, λ_e, and λ_h values of the corresponding polymer were investigated by the extrapolation technique [98], which has been successfully employed to investigate several series of polymers [38, 39, 99–105]. Figure 4 presents the plots of HOMO, LUMO, E_g, λ_{max}, λ_e, and λ_h values for **4a–f** as functions of reciprocal chain length for their corresponding oligomers, with assumed linear extrapolation to infinite chain length. Good linear relationships are found. The corresponding values are listed in Tables S7 and S8 (see the Supporting Information). The extrapolated HOMO, LUMO, E_g, λ_{max}, λ_e, and λ_h values to the infinite chain length are −4.57, −2.62, 1.95 eV, 780.17 nm, 0.008, and 0.015 eV, respectively. These results reveal that increasing the conjugation length of side fragments results in higher HOMO and lower LUMO energies, smaller E_g, λ_e, λ_h, and larger λ_{max} values. This situation was also found in earlier theoretical investigation [106].

Polythiophene is one of the best π-conjugation systems in organic electronic devices and molecular electronics as mentioned above; thus, the E_g, λ_{max}, λ_e, and λ_h values of corresponding polymer of oligothiophene (see Scheme S2, Supporting Information) were also calculated by extrapolation for comparison. The results are shown in Fig. S5 (see the Supporting Information). The predicted E_g, λ_{max}, λ_e, and λ_h values of polythiophene are 2.11 eV, 529.14 nm, 0.173, and 0.212 eV, respectively. In comparison with the corresponding results of polythiophene, our designed polymer has smaller E_g, λ_e, λ_h, and larger λ_{max} values than those of polythiophene, suggesting it to be a good candidate in solar cell, due to its narrower band gap, broader absorption region, and higher charge transfer rate.

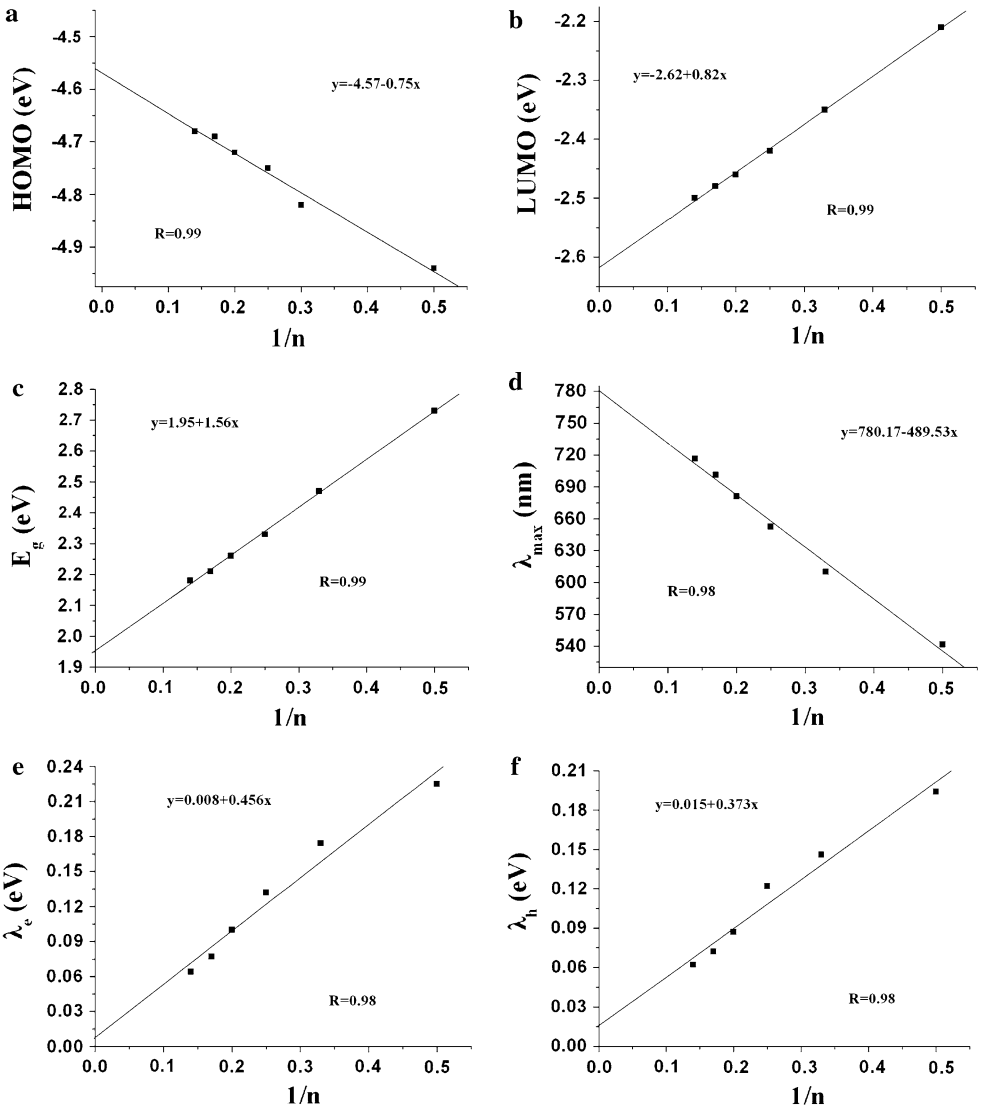

Fig. 4 **a** HOMO; **b** LUMO; **c** E_g; **d** λ_{max}; **e** λ_e; **f** λ_h as a function of 1/n in **4a–f**, where *n* is the number of the repeating units along the polymer chain

4 Conclusions

In the present work, we predicted the optical and electronic properties for a number of OT and OTV derivatives. They were investigated by means of quantum chemical method on the basis of the DFT-PBE0/6-31G(d,p) method. These results show that the two different molecular shapes play a key role in changing the FMOs energies. The V-shape OT derivative with meta-substituted phenyl ring will increase the E_g value because of the meta-substitution resulting in poor conjugation. The absorption spectra were evaluated at the TD-PBE0/6-31+G(d,p) level. Among the investigated molecules **1a**–**3c**, linear OTV derivative with phenyl ring as end-capped group (**2b**) owns the largest λ_{max} value (about 557.51 nm), which is in good agreement with the results of FMOs energies. The reorganization energies of the derivatives were also investigated on the basis of the B3LYP/6-31G(d,p) energies. The V-shape OTV derivative with meta-substituted phenyl as core (**2c**) provides the smallest reorganization energy among the investigated molecules **1a**–**3c**. Additionally, all the investigated molecules have better hole- and electron-transporting balance and can act as nice ambipolar materials. Using theoretical methodologies, it is possible to predict reasonable optical and electronic properties of the OT and OTV derivatives. On the basis of investigated results, we proposed a rational way for the design of charge transport and/or solar cell materials that the promising candidates should possess 1,2,4-phenyl core and longer OTV side fragments. The calculated results by extrapolation reveal that our designed polymer will possess better optical and electric properties than the well-known polythiophene. This study should be helpful in further theoretical investigations on such kind of systems and also to the experimental study for charge transport and/or solar cell materials.

Acknowledgments Financial supports from the NSFC (Nos. 50873020 and 20773022) and the Fundamental Research Funds for the Central Universities are gratefully acknowledged.

References

1. Friend RH, Gymer RW, Holmes AB, Burroughes JH, Marks RN, Taliani C, Bradley DDC, Dos Santos DA, Brédas JL, Lögdlund M, Salaneck WR (1999) Nature 397:121
2. Forrest SR (2004) Nature 428:911
3. Shirota Y (2005) J Mater Chem 15:75
4. Currie MJ, Mapel JK, Heidel TD, Goffri S, Baldo MA (2008) Science 321:226
5. Thompson BC, Fréchet JMJ (2008) Angew Chem Int Ed 47:58
6. Günes S, Neugebauer H, Sariciftci NS (2007) Chem Rev 107:1324
7. Miyata S, Nalwa HS (1997) Organic electroluminescent materials and devices. Gordon and Breach, New York
8. Kraft A, Grimsdale AC, Holmes AB (1998) Angew Chem Int Ed 37:402
9. Mitschke U, Bäuerle P (2000) J Mater Chem 10:1471
10. Kafafi ZH (2005) Organic electroluminescence. Taylor and Francis, New York
11. Müllen K, Scherf U (2006) Organic light-emitting devices, synthesis, properties, and applications. Wiley-VCH, Weinheim
12. Spanggaard H, Krebs FC (2004) Sol Energy Mater Sol Cells 83:125
13. Sun SS, Sariciftci NS (2005) Organic photovoltaics, mechanisms, materials and devices. CRC Press, New York
14. Walzer K, Maennig B, Pfeiffer M, Leo K (2007) Chem Rev 107:1233
15. Mutolo KL, Mayo EI, Rand BP, Forrest SR, Thompson ME (2006) J Am Chem Soc 128:8108
16. Grimsdale AC, Chan KL, Martin RE, Jokisz PG, Holmes AB (2009) Chem Rev 109:897
17. Katz HE, Bao ZN, Gilat SL (2001) Acc Chem Res 34:359
18. Dimitrakopoulos CD, Malenfant PRL (2002) Adv Mater 14:99
19. Katz HE (2004) Chem Mater 16:4748
20. Sun YM, Liu YQ, Zhu DB (2005) J Mater Chem 15:53
21. Mas-Torrent M, Rovira C (2006) J Mater Chem 16:433
22. Kim JY, Lee K, Coates NE, Moses D, Nguyen TQ, Dante M, Heeger AJ (2007) Science 317:222
23. Brédas JL, Norton JE, Cornil J, Coropceanu V (2009) Acc Chem Res 42:1691
24. Heremans P, Cheyns D, Rand BP (2009) Acc Chem Res 42:1740
25. Fichou D (2000) J Mater Chem 10:571
26. Mc Cullough RD (1998) Adv Mater 10:93
27. Fichou D (1999) Handbook of Oligo- and Polythiophenes. Wiley-VCH, Weinheim
28. Müllen K, Wegner G (1998) Electronic materials: the oligomer approach. Wiley-VCH, Weinheim
29. Yang JH, Garcia A, Nguyen TQ (2007) Appl Phys Lett 90:103514
30. Tang WH, Ke L, Tan LW, Lin TT, Kietzke T, Chen ZK (2007) Macromolecules 40:6164
31. Yang XD, Wang LJ, Wang CL, Long W, Shuai ZG (2008) Chem Mater 20:3205
32. Lloyd MT, Anthony JE, Malliaras GG (2007) Mater Today 10:34
33. Roncali J (2009) Acc Chem Res 42:1719
34. Wang Y, Zhou EJ, Liu YQ, Xi HX, Ye SH, Wu WP, Guo YL, Di C, Sun YM, Yu G, Li YF (2007) Chem Mater 19:3361
35. Huang Y, Wang Y, Sang GY, Zhou EJ, Huo LJ, Liu YQ, Li YF (2008) J Phys Chem B 112:13476
36. Chen LP, Zhu LY, Shuai ZG (2006) J Phys Chem A 110:13349
37. Ma J, Li SH, Jiang YS (2002) Macromolecules 35:1109
38. Zhang GL, Ma J, Jiang YS (2003) Macromolecules 36:2130
39. Zhang GL, Ma J, Wen J (2007) J Phys Chem B 111:11670
40. Zhang GL, Pei Y, Ma J, Yin KL, Chen CL (2004) J Phys Chem B 108:6988
41. Meng SC, Ma J (2008) J Phys Chem B 112:4313
42. Meng SC, Ma J, Jiang YS (2007) J Phys Chem B 111:4128
43. Mishra A, Ma CQ, Bäuerle P (2009) Chem Rev 109:1141
44. Tang CW, Van-Slyke SA (1987) Appl Phys Lett 51:913
45. Baldo MA, O'Brien DF, You Y, Shoustikov A, Sibley S, Thompson ME, Forrest SR (1998) Nature 395:151
46. Garnier F, Hajlaoui R, Yassar A, Srivastava P (1994) Science 265:1684
47. Sirringhaus H, Brown PJ, Friend RH, Nielsen MM, Bechgaard K, Langeveld-Voss BMW, Spiering AJH, Janssen RAJ, Meijer EW, Herwig P, de Leeuw DM (1999) Nature 401:685
48. Sariciftci NS, Smilowitz L, Heeger AJ, Wudl F (1992) Science 258:1474

49. Halls JJM, Walsh CA, Greenham NC, Marseglia EA, Friend RH, Moratti SC, Holmes AB (1995) Nature 376:498
50. Nelson J, Kwiatkowski JJ, Kirkpatrick J, Frost JM (2009) Acc Chem Res 42:1768
51. Sitha S, Srinivas K, Raghunath P, Bhanuprakash K, Jayathirtha RV (2005) J Mol Struc Theochem 728:57
52. Raghunath P, Ananth Reddy M, Gouri C, Bhanuprakash K, Jayathirtha Rao V (2006) J Phys Chem A 110:1152
53. Xiao HB, Shen H, Lin YG, Su JH, Tian H (2007) Dyes Pigm 73:224
54. Marcus RA (1993) Rev Mod Phys 65:599
55. Marcus RA, Eyring H (1964) Annu Rev Phys Chem 15:155
56. Hush NS (1958) J Chem Phys 28:962
57. Liu YL, Feng JK, Ren AM (2008) J Phys Chem A 112:3157
58. Frisch MJ, Trucks GW, Schlegel HB, Scuseria GE, Robb MA, Cheeseman JR, Montgomery JAJ, Vreven T, Kudin KN, Burant JC, Millam JM, Iyengar SS, Tomasi J, Barone V, Mennucci B, Cossi M, Scalmani G, Rega N, Petersson GA, Nakatsuji H, Hada M, Ehara M, Toyota K, Fukuda R, Hasegawa J, Ishida M, Nakajima T, Honda Y, Kitao O, Nakai H, Klene M, Li X, Knox JE, Hratchian HP, Cross JB, Bakken V, Adamo C, Jaramillo J, Gomperts R, Stratmann RE, Yazyev O, Austin AJ, Cammi R, Pomelli C, Ochterski JW, Ayala PY, Morokuma K, Voth GA, Salvador P, Dannenberg JJ, Zakrzewski VG, Dapprich S, Daniels AD, Strain MC, Farkas O, Malick DK, Rabuck AD, Raghavachari K, Foresman JB, Ortiz JV, Cui Q, Baboul AG, Clifford S, Cioslowski J, Stefanov BB, Liu G, Liashenko A, Piskorz P, Komaromi I, Martin RL, Fox DJ, Keith T, Al-Laham MA, Peng CY, Nanayakkara A, Challacombe M, Gill PMW, Johnson B, Chen W, Wong MW, Gonzalez C, Pople JA (2004) Gaussian 03, revision B.05, Gaussian 03, revision B.03, Gauss view 3.0. Gaussian, Inc, Wallingford
59. Parr RG, Yang W (1989) Density functional theory of atoms and molecules. Oxford University, Oxford
60. Adamo C, Barone V (1999) J Chem Phys 110:6158
61. Ernzerhof M, Scuseria GE (1999) J Chem Phys 110:5029
62. Hariharan PC, Pople JA (1974) Mol Phys 27:209
63. Gordon MS (1980) Chem Phys Lett 76:163
64. Frisch MJ, Pople JA, Binkley JS (1984) J Chem Phys 80:3265
65. Gahungu G, Zhang B, Zhang JP (2007) J Phys Chem C 111:4838
66. Jacquemin D, Perpète EA (2006) Chem Phys Lett 429:147
67. Perpète EA, Preat J, André JM, Jacquemin D (2006) J Phys Chem A 110:5629
68. Jacquemin D, Wathelet V, Perpète EA (2006) J Phys Chem A 110:9145
69. Jacquemin D, Preat J, Wathelet V, Fontaine M, Perpète EA (2006) J Am Chem Soc 128:2072
70. Azumi R, Götz G, Debaerdemaeker T, Bäuerle P (2000) Chem Eur J 6:735
71. Stratmann RE, Scuseria GE, Frisch MJ (1998) J Chem Phys 109:8218
72. Bauernschmitt R, Ahlrichs R (1996) Chem Phys Lett 256:454
73. Casida ME, Jamorski C, Casida KC, Salahub DR (1998) J Chem Phys 108:4439
74. Jacquemin D, Perpète EA, Ciofini I, Adamo C (2009) Acc Chem Res 42:326
75. Barone V, Polimeno A (2007) Chem Soc Rev 36:1724
76. Gordon MS (1980) Chem Phys Lett 76:163
77. Frisch MJ, Pople JA, Binkley JS (1984) J Chem Phys 80:3265
78. Cossi M, Barone V (2000) J Chem Phys 112:2427
79. Miertuš S, Scrocco E, Tomasi J (1981) Chem Phys 55:117
80. Miertuš S, Tomasi J (1982) Chem Phys 65:239
81. Cossi M, Barone V, Camni R, Tomasi J (1996) Chem Phys Lett 255:327
82. Becke AD (1993) J Chem Phys 98:5648
83. Kim EG, Coropceanu V, Gruhn NE, Sánchez-Carrera RS, Snoeberger R, Matzger AJ, Brédas JL (2007) J Am Chem Soc 129:13072
84. Lin BC, Cheng CP, You ZQ, Hsu CP (2005) J Am Chem Soc 127:66
85. Gruhn NE, da Silva Filho DA, Bill TG, Malagoli M, Coropceanu V, Kahn A, Brédas JL (2002) J Am Chem Soc 124:7918
86. Hutchison GR, Ratner MA, Marks TJ (2005) J Am Chem Soc 127:2339
87. Köse ME, Mitchell WJ, Kopidakis N, Chang CH, Shaheen SE, Kim K, Rumbles G (2007) J Am Chem Soc 129:14257
88. Zou LY, Ren AM, Feng JK, Liu YL, Ran XQ, Sun CC (2008) J Phys Chem A 112:12172
89. O'Boyle NM, Vos JG (2003) GaussSum 1.0, Dublin city University
90. Forés M, Duran M, Solà M, Adamowicz L (1999) J Phys Chem A 103:4413
91. Ponomarenko SA, Kirchmeyer S, Elschner A, Alpatova NM, Halik M, Klauk H, Zschieschang U, Schmid G (2006) Chem Mater 18:579
92. Mitchell WJ, Kopidakis N, Rumbles G, Ginley DS, Shaheen SE (2005) J Mater Chem 15:4518
93. Kopidakis N, Mitchell WJ, Van de Lagemaat J, Ginley DS, Rumbles G, Shaheen SE (2006) Appl Phys Lett 89:103524
94. Ran XQ, Feng JK, Ren AM, Li WC, Zou LY, Sun CC (2009) J Phys Chem A 113:7933
95. Irfan A, Zhang JP, Chang YF (2009) Chem Phys Lett 483:143
96. Wang CL, Wang FH, Yang XD, Li QK, Shuai ZG (2008) Org Electron 9:635
97. Yang XD, Li QK, Shuai ZG (2007) Nanotechnology 18:424029
98. Lahti PM, Obrzut J, Karasz FE (1987) Macromolecules 20:2023
99. Wang JF, Feng JK, Ren AM, Liu XD, Ma YG, Lu P, Zhang HX (2004) Macromolecules 37:3451
100. Salzner U, Lagowski JB, Pickup PG, Poirier RA (1998) Synth Met 96:177
101. Cornil J, Gueli I, Dkhissi A, Sancho-Garcia JC, Hennebicq E, Calbert JP, Lemaur V (2003) J Chem Phys 118:6615
102. Ford WK, Duke CB, Paton A (1982) J Chem Phys 77:4564
103. Brière JF, Côté M (2004) J Phys Chem B 108:3123
104. Klaerner G, Miller RD (1998) Macromolecules 31:2007
105. Rathore R, Abdelwahed SH, Guzei IA (2003) J Am Chem Soc 125:8712
106. Zhang YX, Cai X, Bian YZ, Li XY, Jiang JZ (2008) J Phys Chem C 112:5148